INSTRUMENTATION

Seven-Pinhole Multigated Tomography and Its Application to Blood-Pool Imaging: Technical Parameters

Wei Chang and Robert E. Henkin

Foster G. McGaw Hospital–Loyola University Medical Center, Maywood, Illinois

The application of seven-pinhole tomography has been predominantly to thallium-201 myocardial imaging. In view of the stationary nature of the collimator, with all views accumulating simultaneously, seven-pinhole tomography can be adapted to dynamic cardiac imaging, namely, multigated blood-pool imaging. Existing reconstruction software was modified to process the gated blood-pool data. The performance parameters of the seven-pinhole system were investigated at Tc-99m energy. This work provides an additional understanding of the seven-pinhole system as well as its potential application to abnormalities of ventricular wall motion or the quantitation of other cardiac parameters from reconstructed data.

J Nucl Med 21: 682–688, 1980

The introduction of seven-pinhole tomography by Vogel et al. has been received with enthusiasm (*1*). Early work has suggested that the application of this technique to Tl-201 imaging will increase the sensitivity and specificity of the diagnosis of coronary artery disease (*2*). Complementary information about cardiac function is derived from multigated equilibrium blood-pool studies (MUGA). A natural extension of the seven-pinhole approach is to apply it to MUGA studies. With the application of tomography to MUGA data, it was expected that the ventricular walls would be better delineated at depth due to the defocusing effect of the foreground and background activities.

During Tc-99m-labeled blood-pool imaging, there is a much higher photon flux than in Tl-201 myocardial perfusion imaging. This abundance of photons makes *multigated tomography* (*MUGTM*) feasible.

The performance characteristics of the seven-pinhole collimator system are not widely disseminated. Before proceeding to extensive clinical studies, we elected to study the collimator system. Our results, with comments and sample clinical studies, are presented here.

Received Jan. 2, 1980; revision accepted March 24, 1980.

For reprints contact: W. Chang, PhD, Dept. of Nuclear Medicine, Loyola Univ. Medical Ctr, 2160 S. First Ave., Maywood, IL 60153.

MATERIALS AND METHODS

A commercial seven-pinhole collimator* was used to acquire data on a large-field camera.† A fully programmable, dedicated minicomputer system was interfaced to the camera to store the data and then reconstruct the tomograms.‡

Clinical data were acquired in the 45° LAO projection. A typical example of the unprocessed images is shown in Fig. 1. The left ventricle is in the center of each of the seven-pinhole images and occupies as much of the field of view as possible. The computer's acquisition cycle was synchronized with the patient's R wave through a physiologic trigger.‖ Three 14-frame MUGA series, in a 64- × 64-byte mode, were acquired with the acquisition software provided with the computer. The average number of counts per frame was specified to be 125,000 in each series. This method of acquisition has no count-rate limitation and has an automatic restart option at the end of each series. The only reason for acquiring multiple sequential studies is to achieve statistically reliable reconstruction without overflowing the storage capacity in byte-mode acquisition.

To achieve proper uniformity correction and establish a reference depth calibration, images of a flood and point source were obtained using Tc-99m sources. These data were handled in a fashion similar to that of Tl-201 calibration (*1*).

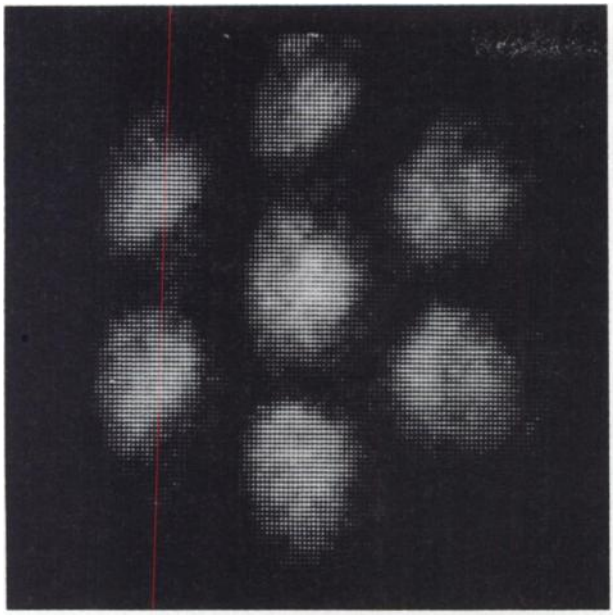

FIG. 1. Single-frame unreconstructed image of LAO gated blood-pool study acquired with seven-pinhole collimator. Image was originally acquired in 64 × 64 matrix, then linearly interpolated to 128 × 128 for processing.

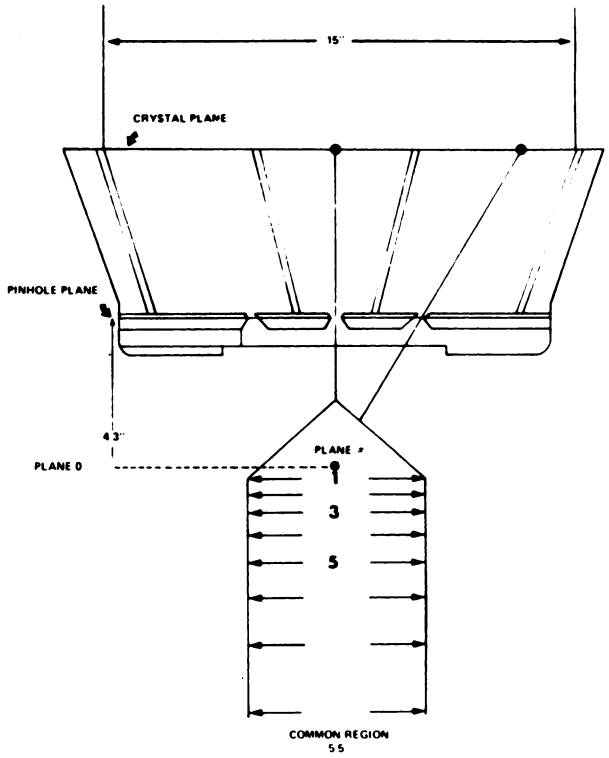

FIG. 2. Lateral view of seven-pinhole collimator and its geometric relation to focused planes, with plane numbers as defined in text (courtesy of CMS Corp.).

For convenience in the following discussion, each focused plane is identified with a number. The plane normal to the central axis of the collimator and 11.0 cm from it (the distance used for the reference point source during the calibration procedure) will be identified as the focused Plane 0, as no matrix shift in relation to the calibration point source is needed to reconstruct the image of this particular plane. Every two-pixel shift of the six peripheral views toward the central axis of the collimator creates the next focused plane, with a corresponding increase of one in plane number. Figure 2 shows the relations between these focused planes. As the plane number increases, the corresponding depth of the plane also increases. A negative plane number indicates that the shift is in a direction closer to the collimator than the reference depth. However, the effective field of view for these closer planes is often too close and/or too small to be useful in cardiac imaging.

Depth and resolution measurements. A clock phantom,§ 5 in. in diameter and filled with Tc-99m, was imaged and reconstructed in this system (*3*). This phantom permits the determination of the depth of each reconstructed focused plane. Because each focused plane is perpendicular to the axis of the cylinder, it should intersect the double helix at two points exactly 180° apart. The angle of rotation of a line connecting the two in-focus points in one plane, as compared with a line connecting the two in-focus points in another plane, is a measure of the distance between the two planes. After the depth of each focused plane was established, the planar and depth resolutions were measured with a line source (1-mm capillary tube filled with Tc-99m) in air for several planes. The capillary tube was located at the center of the field, at depths corresponding to focused Planes 1, 3, and 5. The objects in these experiments were stationary, therefore, 128 × 128 matrices were used for acquisition instead of the 64 × 64 matrix used for blood-pool studies.

Oscillating clinical studies and phantom. After the three 14-frame series of MUGA data were acquired and stored as described above, reconstructions were performed. The existing reconstruction software was modified to accept data in the 64 × 64 byte mode by using a linear interpolation and adding instructions enabling the software to loop back for the reconstruction of the succeeding frames.

To simulate the clinical situation, an oscillating phantom was constructed (Fig. 3). A standard thyroid phantom was placed in air, 5 cm above the two angled line sources on a platform that oscillated in 3-cm single harmonic motion during data acquisition. Each time the oscillating phantom moved to the minimum-displacement position, a microswitch was closed and a 5-volt square wave was sent to the computer to simulate an R wave.

In the clinical situation, an average of 375K counts per frame was acquired over 5–8 min, in an LAO projection. Studies were initially performed with a 4.5-mm pinhole.

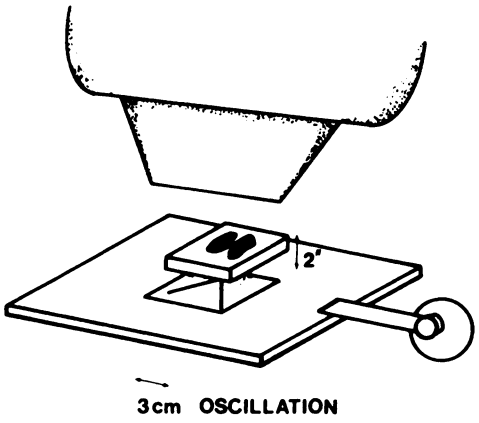

FIG. 3. Oscillating phantom consists of standard thyroid phantom suspended in air 5 cm above two line sources that lie on oscillating platform moving in simple harmonic motion with 3-cm excursion.

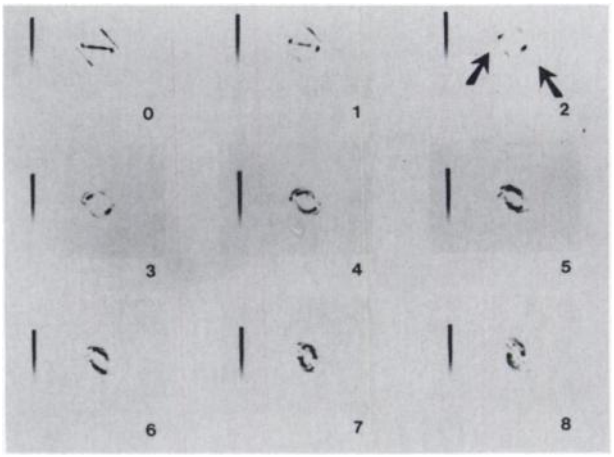

FIG. 4. Reconstructed clock-phantom images (Planes 0–8). Two opposite focused points, as indicated by arrows on Plane 2, start rotating clockwise as the plane number increases.

The 5.5-mm pinhole proved to be 30% more sensitive and ultimately replaced the smaller pinhole.

RESULTS

Depth and resolution measurements. Nine consecutive planes (Planes 0–8) were reconstructed from a clock phantom and are shown in Fig. 4. In the first several images, the reconstructed plane intersects the double helix (the lines of activity) at two opposite points that are relatively well focused. On deeper planes (Planes 4 and 5) the "points" of intersection are not as well focused and there is "tailing" on either side of the focused points. For the very deep planes (Planes 6–8), it becomes very difficult to determine exactly where the focused plane (or the intersecting points) might be. These images demonstrate that not only does the depth resolution deteriorate on deeper planes, but also the reconstructed "tomograms" are far less useful tomographically beyond a certain depth (more than 20 cm from the collimator face). The diameter of the helical cone shrinks on deeper planes, as would be expected from the pinhole geometry. This implies that each plane has its own scaling factor.

A geometric estimation of the plane depth, based on the algorithm employed, was compared with the experimentally determined plane depth as measured from the clock phantom. The estimated and measured depths of the planes, for Planes 0–7, are plotted in Fig. 5. It demonstrates that the reconstructed planes are indeed unevenly spaced, i.e., the distance between each pair of adjacent planes increases as the depth increases. The spacing increases from less than 1 cm (between Planes 0 and 1) to about 3 cm (between Planes 4 and 5) in four steps. However, there is a discrepancy between the estimated depth and measured depth, and it is greater for deeper planes. The uncertainty of the depth of the deep focused planes is demonstrated in Figs. 4 and 5.

The planar and depth resolution data, measured with a Tc-99m line source located at the centers of Planes 1, 3, and 5, respectively, are shown in Fig. 6. The line spread function (LSF) is the profile shown at the center of each of the three families of profiles for the respective focused planes. Because it was focused, such a profile demonstrates a maximum peak and smallest spread. The measured full widths at half maximum (FWHM) are 1.15, 1.3, and 1.6 cm, respectively, on these three planes. The other profiles demonstrate that the shadows of line images are also represented on the adjacent planes, but were defocused to show lower peak values and greater spread in the xy dimension. The profile eventually

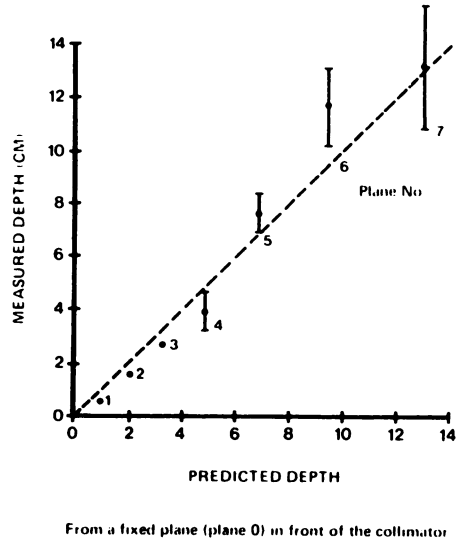

From a fixed plane (plane 0) in front of the collimator

FIG. 5. Plot of measured depth of each focused plane against geometrically predicted depth for large field camera. Gain setting is for 45 pixels between center pinhole image of calibration point source and one of six peripheral point-source images.

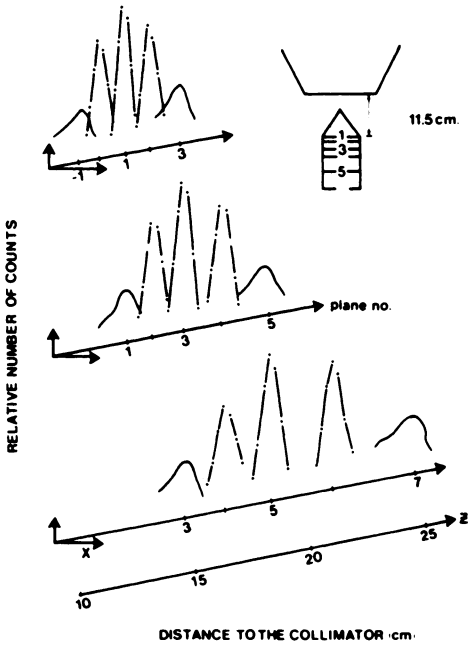

FIG. 6. Planar and depth-resolution data measured with Tc-99m line source located at centers of Planes 1, 3, and 5, respectively.

smoothes out into the background.

The envelopes of each family of profiles are the corresponding depth (z axis) LSFs on these three planes. Table 1 lists the experimental FWHMs of these planar and depth LSFs at the center of these three planes. The depth resolutions, FWHM, are 3.6, 4.8, and 8.3 cm, respectively.

Oscillating phantom and clinical studies. The reconstructed multiframe tomograms of the oscillating phantom can be replayed in a cine format. Figure 7 shows the simulated end-diastole (ED) and end-systole (ES) frames at two focused planes corresponding to the depths of the two phantoms. Note an artifact indicated by the arrow in Fig. 7. The origin of this artifact will be discussed later.

A typical patient's blood-pool tomogram in 45° LAO view is shown in Fig. 8 at two depths. Every other frame of a 14-frame series of a cardiac cycle is shown, with the Series 8A representing Plane 2 and Series 8B representing the deeper Plane 5.

The images are, as expected, smoother than the nontomographic images due to the heavy data manipulation. The ventricle has a well-defined edge and shows differences in shape at the two depths. Edge definition is primarily enhanced by the focal-plane tomographic technique.

TABLE 1. FWHM (CM) OF THE LSF ON SEVERAL PLANES IN FRONT OF THE PINHOLE PLATE*

	Plane number		
	1	3	5
Depth	11.5	13.7	18.7
x-y FWHM	1.15	1.3	1.6
z FWHM	3.6	4.8	8.3

* The Tc-99m line-source images were acquired in 64 × 64 matrix with 5.5-mm pinhole on an LFOV camera. Linear interpolation was applied before reconstruction.

DISCUSSION

The combination of seven-pinhole tomography with a multigated blood-pool study suggests that better visualization of the ventricular wall at multiple specified depths may be obtained on MUGTM studies than on nontomographic gated studies. More extensive clinical studies are under way.

In the case of seven-pinhole tomography, the six peripheral views provide the depth information. This is best illustrated by the reconstructed image of a point source. When it is in focus, the seven subimages overlap right on top of each other and show a sharply focused image of a point source. When it is not in focus, the six peripheral components drift outward from the center one. The amount of drift is proportional to the degree of defocusing. In other words, the blurring pattern is just an image of the pinholes, with the pattern's dimensions proportional to the distance between the reconstructed plane and the point source itself. This is typical of this kind of focal-plane tomography (*4*). Compared with other kinds of coded-aperture tomography, the difference here is that all seven pinholes are in simultaneous and continuous operation and all seven views are well sepa-

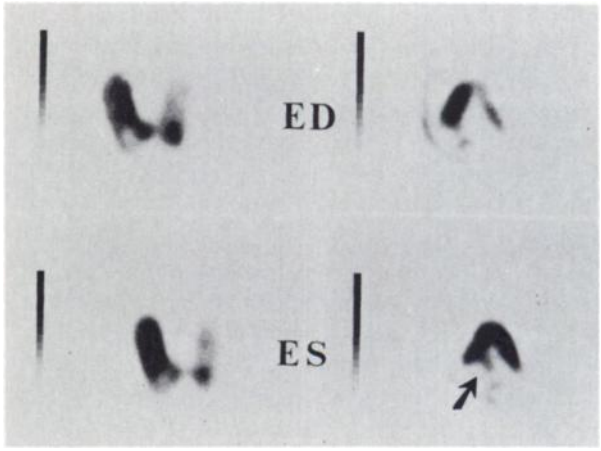

FIG. 7. Simulated ED and ES frames of oscillating phantom at two depths (Planes 2 and 5) which are focused planes of two sources. Multigated images were acquired during phantom oscillation. Artifact on deeper plane indicated by arrow is caused by the shadow of activity on the other plane and difference in scaling factors for these two planes. Dotted blank pixels on images are artifacts caused by our display hardware.

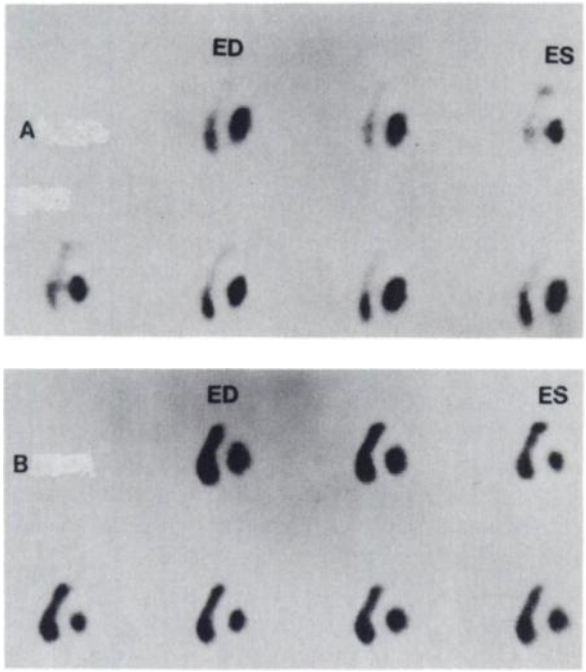

FIG. 8. Reconstructed blood-pool tomograms (for illustration purposes, only every other one of 14 frames is shown). (A) Series representing a cardiac cycle on Plane 2. (B) Series representing a cycle on a deeper Plane 5.

rated. These features allow fast back-projection to be employed (MT LeFree, et al., personal communication).

All the static images for the performance tests were acquired in 128 × 128 matrix. However, our clinical images were limited to the 64 × 64 matrix size, which was followed by interpolation to 128 × 128 before the reconstruction took place. The use of a finer acquisition matrix in the measurement of performance parameters can yield a value with less uncertainty. For all practical purposes, the performance parameters acquired in the 128 × 128 matrix agree closely with the 64 × 64 matrix acquisition and interpolation. Table 2 compares the FWHMs obtained with the two matrix sizes and two pinhole diameters. The differences are too small to be appreciated in cardiac imaging even in a multigated situation.

From the results with the clock phantom, it is confirmed that the depths of the reconstructed planes are unevenly spaced for this version of software, which is based on the shift algorithm of a fixed number of pixels. This is a result of the pinhole geometry, because the same amount of matrix shift in the reconstruction of tomograms would correspond to progressively larger increments in the depth of each focused plane. In other words, each pixel located close to the central axis of the collimator in the peripheral views covers a larger range of depth information than a peripheral pixel in the same view.

Other versions of reconstruction software have the

TABLE 2. FWHM (CM) OF THE Tc-99m LSF WITH TWO ACQUISITION MATRICES AND PINHOLE SIZES

Acquisition matrix	Pinhole diameter (mm)	
	4.5	5.5
64 × 64	1.15	1.2
128 × 128	1.05	1.15

option of reconstructing evenly spaced tomograms. Although it is easier to visualize a three-dimensional image from evenly spaced tomograms, such a process may also introduce potential problems. Since the evenly spaced planes are a result of an interpolation process, the information content remains the same. However, the interpolation process has to be based on a precise knowledge of the depth of each original focused plane. The increasing uncertainty of plane depth in the z dimension is inherent in the current system and is also closely related to the linearity of the gamma camera, which not only varies from camera to camera but also may change with time in the same camera. Therefore, unless one really calibrates the spacing between adjacent planes with known geometry on a daily basis, the interpolated results can potentially misrepresent the true three-dimensional picture.

From the planar FWHM measurements at the centers of Planes 1, 3, and 5 mentioned above, the planar resolution (xy axis) remains quite good throughout the deep planes. Within the same family of profiles of a line source, the shadow of the source on the adjacent planes is quite significant. This phenomenon is also reflected in the measurements of depth resolution (z axis). The magnitude of the shadow depends on the distance between the planes and on the strength of the activity in question. Clinically, therefore, a lesion of either increased or decreased photon flux in one plane may be represented significantly in "adjacent" planes. The artifact in Fig. 7 is the combined effect of the shadow and the different scaling factors for the two planes. This can cause a potential problem in the imaging of a high-contrast object. In addition, the measurements of depth resolution (z axis) indicate that the FWHM increases rapidly with plane depth. This implies that the tomographic effect is less pronounced for the deep planes than for the closer planes.

From geometrical considerations, one can demonstrate that, on the same plane, the z-depth resolution is not uniform throughout the effective field of view, but rather gradually improves as one moves away from the central axis. The change of depth resolution is symmetrical with respect to the central axis and makes the measurement of LSF difficult for an off-axis location. Theoretically, a point source can better serve the purpose

of measurement of resolution. There are some practical difficulties associated with the measurement of a point-source spread function (PSF), especially with an acquisition matrix that is limited in both size and capacity. Nevertheless, another group has reported comparable planar resolution but better depth resolution at these depths (MT LeFree, et al., personal communication). The location of their PSF experiment was half way between the edge and the central axis of the common field of view (Dennis Kirch, personal communication, 1979).

In the case of thallium or blood-pool imaging, the critical area of the image (the myocardium or the ventricular wall) is usually located peripherally and symmetrically around the central axis of the field. Therefore, the tomographic effect on the region of interest should be better than our depth-resolution measurements imply.

The slight discrepancy between the estimated depth and the measured depth in Fig. 5 for the first several planes may be attributed to experimental error. In the deeper planes, the discrepancy becomes more serious and the uncertainty of these depths is particularly disturbing.

For the very deep planes (Planes 6–8), not only does the depth become uncertain, but the depth resolution deteriorates further and becomes inadequate. There are at least two major reasons for this problem. First is the finite size of the pinhole and the pixels of the matrix. The matrix after interpolation, 128 × 128, is still too coarse to reconstruct a very deep tomogram. Among the six peripheral views of the acquired image, only two are really following the "two-pixel shift algorithm" down to the very deep planes. The other four side views are shifting at an angle with respect to the x axis of the image matrix. This fact causes an inherent error in reconstruction. The problem becomes more and more critical for the deep tomograms; thus the deep tomograms are not really focused in "one" particular plane. This leads directly to the uncertainty of depth and poor depth resolution for the corresponding tomogram. Even a perfect interpolation scheme, devised for a precise amount of matrix shift, will still suffer from the same problem, although to a lesser extent, due to the discrete nature of the sampled information. An analog reconstruction with optical equipment may obviate this problem (*5*).

A more significant reason further compounding the uncertainty of the depth of deep planes results from the camera's nonlinearity. The geometrical estimation of plane depth is based on the assumption of perfect camera linearity, which is not the case. It has become obvious that camera linearity is the most important performance parameter in this kind of multisegmental collimator tomography (*6*). Even with cameras having good spatial resolution but poor linearity, one cannot produce good-quality tomograms and may potentially cause artifacts.

We cannot overemphasize the importance of patient positioning with respect to the collimator. The patient's heart should be placed as close to the collimator as possible, while at the same time each of the seven views should cover the whole object of interest in its own field.

From the multigated studies of the oscillating phantom and the patient studies shown above, we find that tomographic blood-pool imaging is clinically practicable and the images are adequate for a limited range of depth (e.g., Planes 0–5).

This kind of focal-plane tomography in combination with the pinhole collimator's response has its advantages as well as its limitations. We believe one should have an idea of a new system's performance parameters before applying it clinically. Also, these parameters vary with each individual camera's performance. Both the intrinsic resolution and linearity of the camera are therefore critical in producing adequate tomograms. Quality control of the camera's performance is essential.

We feel that there is room for the collimator design to be optimized for each application. For example, sensitivity, resolution, field size, and angulation of the pinhole, etc., should be designed for the organ to be imaged and be clinically practical to perform.

The reconstruction of a 14-frame MUGA series originally took 2.5 hr but has recently been reduced to 20 min. After the clinical efficacy and software optimization have been established, the reconstruction time can be shortened further.

In conclusion, we have shown that tomographic gated blood-pool studies are feasible in a clinical situation and have adequate technical performance parameters in its effective range. Further development is necessary to refine this technique, which potentially offers further quantitation of regional left-ventricle performance. Early results of patient studies will be presented separately.

FOOTNOTES

* CMS Scintislice Collimator.

† Searle LFOV camera with 3/8 in. crystal.

‡ MDS Modumed with Tricam software.

‖ Brattle Physiological Synchronizer.

§ Clock phantom was originally designed for Searle's tomographic scanner (Pho/Con). It is a single line source formed like a double helix on a cylindrical surface.

ACKNOWLEDGMENTS

The authors are grateful for the assistance of Barbara Rayunec in preparing the manuscript.

This paper was presented in part at the 26th Annual Meeting of the Society of Nuclear Medicine, held in Atlanta, GA, June, 1979.

REFERENCES

1. VOGEL RA, KIRCH DL, LEFREE MT, et al: A new method

of multiplanar emission tomography using a seven pinhole collimator and an Anger scintillation camera. *J Nucl Med* 19: 648-654, 1978

2. VOGEL RA, KIRCH DL, LEFREE MT, et al: Thallium-201 myocardial perfusion scintigraphy: Results of standard and multi-pinhole tomographic techniques. *Am J Cardiol* 43: 787-793, 1979
3. Pho/Con™ Multiplane Imager System Model 1792 Operation Manual. #710-717680 (Rev. B). Searle Radiographics, Inc, pp 5-32, Oct, 1978
4. ANGER HO: Multiplane tomographic scanner. In *Tomographic Imaging in Nuclear Medicine*. G. S. Freedman, ed. New York, Society of Nuclear Medicine, 1973, pp 2-18
5. BRUNSDEN B, KIRCHNER P, CHARLESTON D, et al: Simple optical back-projection of Kirch collimator (7-pinhole) images for tomography reconstruction. *J Nucl Med* 20: 608, 1979 (abst)
6. KORAL KF, ROGERS WL, KEYES JW, et al: Effect of camera linearity correction upon N-pinhole tomography. *J Nucl Med* 20: 644, 1979 (abst)